Iris Detection and Localization Based on Contrast Shrinking and Stretching of CIELab Color

Susijanto T. Rasmana, Pauladie Susanto, Heri Pratikno
Computer Engineering
Institut Bisnis dan Informatika Stikom, Surabaya, Indonesia
susyanto@stikom.edu, pauladie@stikom.edu, heri@stikom.edu

***Abstract*—Detection and localization are important processes in the effort to segment the iris. In this paper, we present the method for iris detection and localization using Contrast Shrinking and Stretching (CSS). This method was applied to the image in the CIELab color model. From the CIELab color model, the *L** channel was used for iris detection, and *b** channel was used for pupil detection. This method is very suitable applied to the color eye image. Based on the measurement, the accuracy is 95.31%.**

***Keywords*—iris detection; iris localization; CIELab color; contrast shrinking; contrast stretching.**

INTRODUCTION

Iris is a part of the eye that has so far been the topic of biometric and iridology research. Biometric authentication based on iris is very effective for personal identification [1]. Until now biometric using iris is considered to have a high level of security [2], [3]. Iris, in iridology, is used to identifying the patient's health. Iridology research continues to be developed into a valid scientific technique [4].

Detection and localization are the important initial steps for iris research. The iris is the part of the eye that lies between the sclera and the pupil. Proper detection and localization process will affect the results of iris segmentation and recognition. The purpose of this process is to narrow the image from eye area into iris area only.

Various methods offered by the researchers for iris detection and localization, such as integrodifferential operator offered by Daugman [5], this method search for iris circles on the image based on the maximum angular integral of the radial derivative. The second method is offered by Wildes [6]. This method uses Circular Hough Transform (CHT) to detect the iris edge. Another method used for iris localization is Watershed segmentation [7], [8]. Ferone combines Watershed and image quantitation methods [7], and Yan combines Watershed and region merging methods [8].

Image data used for iris detection are generally in the grayscale color model [5], [7]–[9], and some researchers use YCbCr and YIQ color models, such as [10] and [11]. In the proposed method, we use image data in the CIELab Color model. This color model has 3 channels: *L**, *a**, and *b**. *L** represents lightness, *a** represents red and green color, and *b** represents blue and yellow color [12]. CIELab was chosen because it has been successfully used to segment various objects. [13]–[16].

By doing contrast shrinking and stretching on the image in CIELab color model will get iris and pupil areas. The purpose of this study was to find a simple method for detection and localization of iris but effective. Localization was done by limiting the iris area adjacent to the sclera on the outer side and the pupil on the inner side using the circle line. Next, the outer and inner circles can be used for iris segmentation. In this study only discusses the detection and localization and not segmentation.

The iris localization data used is the eye image of the UBIRIS v1 data set, created by University of Beira, Portugal. [17]. Data from UBIRIS was chosen because using the color image (RGB), besides having more information, the RGB image will be changed to CIELab color model.

IRIS LOCALIZATION

Several steps accomplish detecting and localizing of iris by the proposed method as shown in Fig. 1.

A. Smoothing

The first step in the proposed method is smoothing. Smoothing aims to reduce the texture roughness of the iris image. This will make it easier to detect the iris. Smoothing is also used to reduce the noise in the eye image in the form of specular highlights caused by the reflection of light on the eye lens [3]. Smoothing was done using Gaussian Filter, by following formula:

$$G(x,y) = \frac{1}{2\pi\sigma^2} e^{-\frac{x^2+y^2}{2\sigma^2}} \quad (1)$$

Where the value σ = 10. The results of smoothing the eye image with Gaussian blur are presented in Fig. 2.

B. RGB to CIELab color

The next step is to change the image of the smoothing result, from RGB to CIELab color model. Changing the color model from RGB to CIELab uses the equations as used in [14]. In this study, only two of the three CIELab channels were used, that are the *L** and *b** channels. The *L** channel, which represents lightness, is used to detect the iris. Next, the *b** channel, which represents the blue and yellow colors, is used to detect the pupil. The eye images in *L** and *b** channel shown in Fig. 3.

In the *L** channel the iris and pupil areas are relatively darker than other areas. Similarly, eyelashes are relatively darker, but not circular. Contrast shrinking and stretching process will produce the same gray level of iris and pupil area. The *b** channel was used to separate iris and pupil. In the *b** channel, the pupil pixel value is relatively low and looks darker than other areas, whereas iris values are relatively higher and look brighter. Based on that, the two channels will be integrated to localize the iris area.

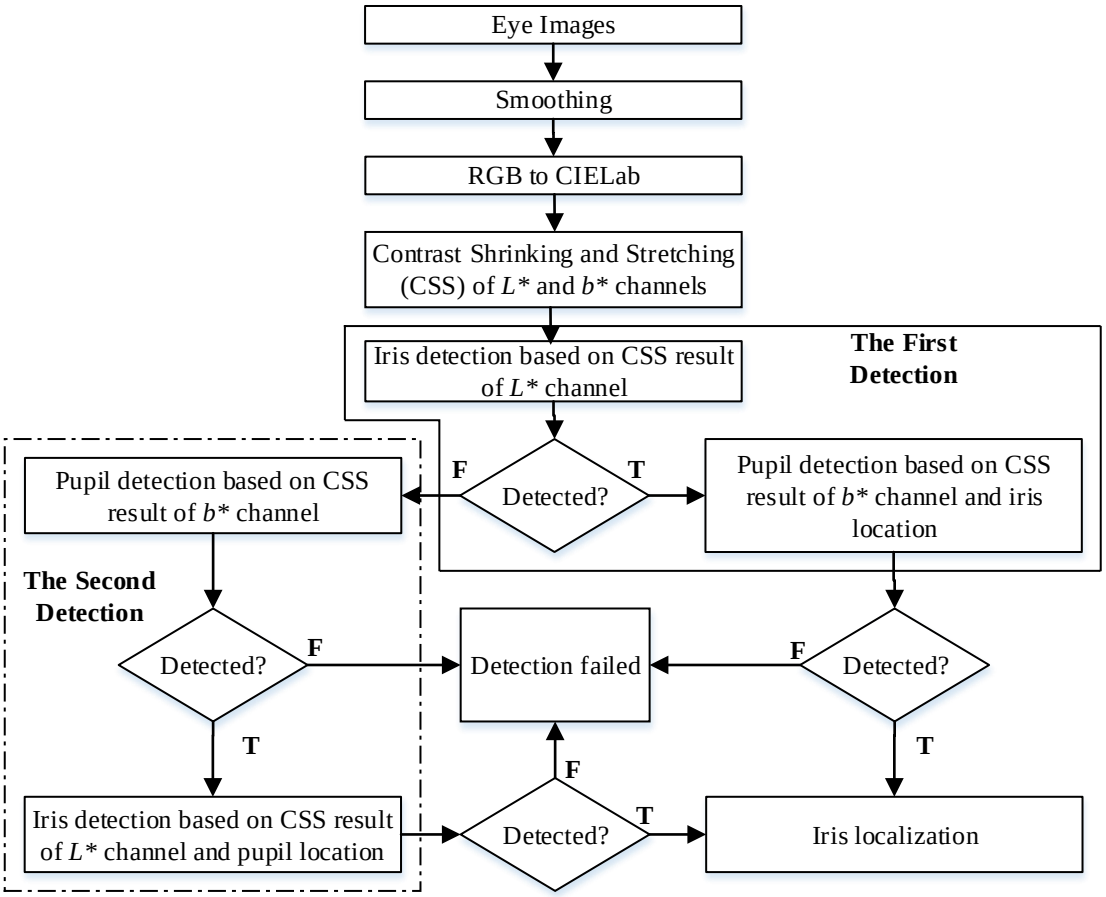

Fig. 1. Block diagram of the iris detection and localization, consists of five steps: smoothing, change from RGB to CIELab color model, contrast shrinking and stretching to L^* and b^* channels, iris and pupil detection (consist two processes), and iris localization.

C. Contrast Shrinking and Stretching

The CSS process consists of two stages: contrast shrinking and contrast stretching. This process was done on L^* and b^* channels. Contrast shrinking aims to narrow the distribution of intensity values and simplifying of intensity values variations. This was done by using Eq. (2).

$$N_{(x,y)} = round\left(\frac{I_{(x,y)}}{\phi}\right) \qquad (2)$$

Where ϕ is the luminosity value, and I is the pixel value of the image. Next, the contrast stretching process, which maps the values obtained to the lower limit and upper limit of grayscale values using Eq. (3).

$$M_{(x,y)} = \frac{N_{(x,y)} - N_{min}}{N_{max} - N_{min}} \times 255 \qquad (3)$$

Where N_{min} and N_{max} are the minimum and maximum values of image pixels, the results of the contrast shrinking process.

The ϕ value used in the contrast shrinking process is different for each eye image. The ϕ values were 70 to 100 for pupil detection and 70 to 200 for iris detection. Detection using the CHT method. Variations of ϕ values were tested sequentially until CHT detects the area of the iris or pupil. Based on the observations, variations of the ϕ values are related to iris color, but this still needs further investigation. The result of the CSS process is then performed thresholding and inverting. Thresholding uses a level value of 0.5. Examples of the CSS outcome are present in Fig. 4.

Fig. 2. Gaussian blurr result on iris image of UBIRIS. v1.

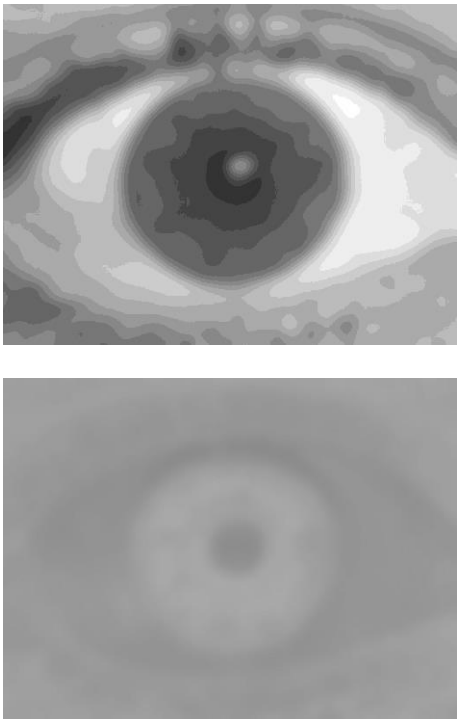

Fig. 3. Eye image in *L** channel (first row) and *b** channel (second row).

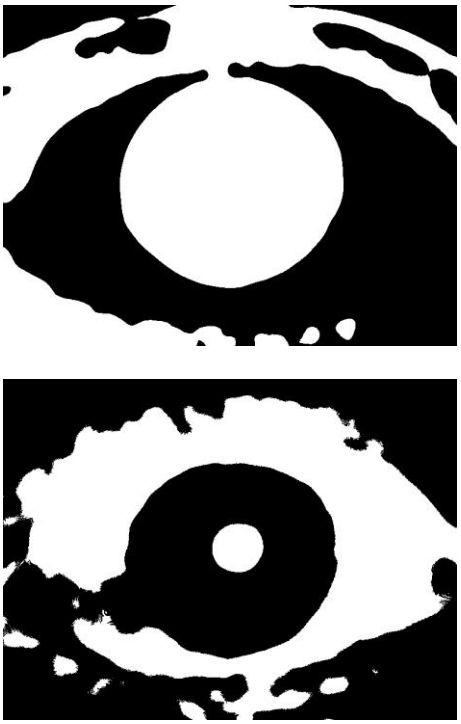

Fig. 4. Eye images after process of contrast shrinking and stretching in *L** channel (first row) and *b** channel (second row).

D. Detection and Localization

There are two detection processes, and each process consists of two stages. The first stage of first process is iris detection and the second stage is pupil detection. As presented in Fig. 1, the first stage of detection is detecting iris in *L** channel based on the CSS output. Detection starts from the iris based on the reason that iris is larger than pupil. Size invariant circle of CHT method was used to pupil detect [18]. If the iris is successfully detected then performed the second stage that is the pupil detection. Detection was done using CSS results in *b** channel by CHT method. In addition, the pupil was detected based on its position within the iris. The pupil position is detected based on the location of the pupil center point and the iris center point. From our measurements on the eye images, the position of the pupil center and the center of the iris is less than 30 pixels. If more than one pupil is detected, it is selected based on the closest distance between the center point of the pupil and the iris, and no more than 30 pixels distance.

If the first detection process fails then a second detection is performed. Based on the experimental results, the cause of failure in the first process of detection due to noise in the iris or most of the iris covered by eyelashes or eyelid. In the first stage of the second detection process, the pupil detection was performed. Differences of the pupil detection in the first and second process are: in the second process, the pupil detection was not based on the iris position, and performed with a lower sensitivity of detection rate. Detection with a low sensitivity aims to make the circle detected by CHT is really a form of the pupil. If the pupil successfully detected then the iris detection is performed based on the pupil position. The second detection of iris uses the same method as in the first detection process but

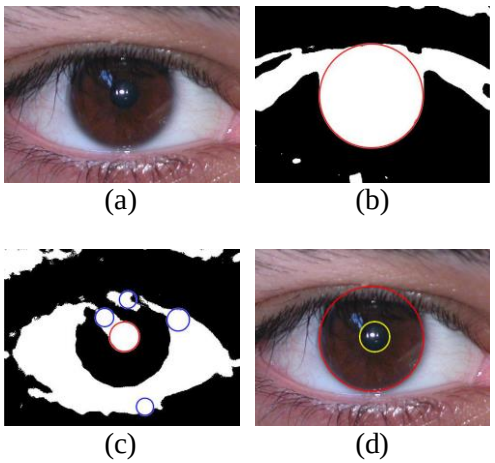

Fig. 5. (a) Eye image with noise specular reflections (data from UBIRIS v1 session 2). (b) Contrast adjustment and thresholding process in *L** channel and (c) in *b** channel, There are several areas detected as the pupil in *b** channel (indicated by several circles) but selected a circle with the midpoint closest to the center of the iris (marked with a red circle), (d) the localization result.

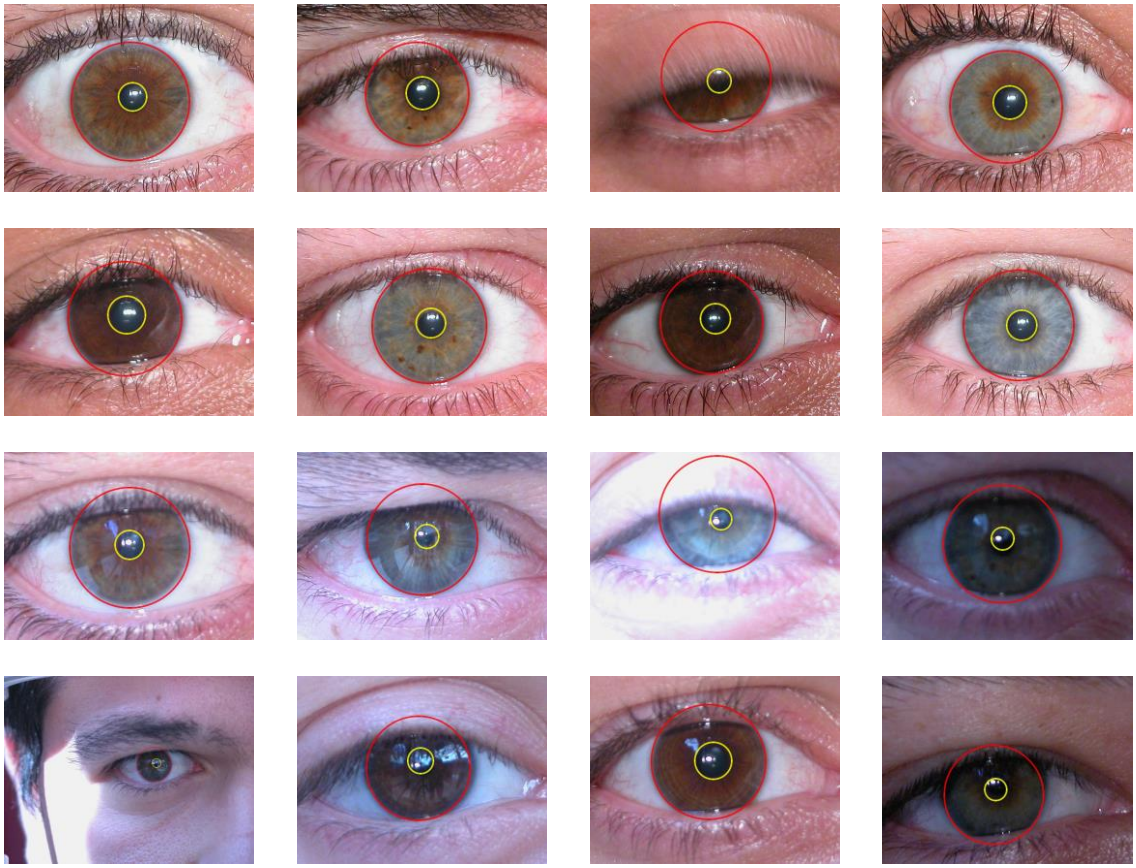

Fig. 6. Some examples of iris detection and localization results. Data uses UBIRIS v1 sessions 1 (first and second rows), and session 2 (third and fourth rows).

with a higher sensitivity level. The risk of increasing this sensitivity is the number of areas detected as iris can be more than one. This problem can be solved by selecting the area detected by CHT, which has the nearest center point to the pupil center point and with a distance fewer than 30 pixels.

The advantage of the proposed method is to detect images that have noise specular reflections (in the UBIRIS v1 session 2), without any preprocessing actions to eliminate them. Specular reflections are a bright spot on the eye image due to the reflection of light in the lens of the eye [20], as shown in Fig. 5 (a). This noise covers the iris image and can thwart the iris detection. In the luminosity adjustment and thresholding process in L^* channel, the specular reflections will not appear (see Fig. 5 (b)). This will make it easier for the iris detect. However, the specular reflections will appear in b^* channel used to detect the pupil as seen in Fig. 5 (c). But, this does not matter, because the noise does not appear when the first detection is done on the L^* channel to detect the iris. Furthermore, pupils are detected based on the shape and the closest distance between the center point of pupil and iris. This method can overcome the problem of disturbed pupil detection due to specular reflections.

The iris area successfully detected then localized with a circle line. There are two circles used, the outer circle and the inner circle. The outer circle is the boundary between iris and sclera, and the inner circle is the boundary between iris and pupil. Some examples of iris localization results are shown in Fig. 6.

Experiments and Results

The proposed method has been tried to detect and localize on all UBIRIS.v1 data sets. The total number of eye images from UBIRIS is 1,877, that taken in two sessions. The first session contains 1214 of good-quality images and the second session contains 663 of images with noise, such as luminosity, defocus, occlusions, and reflections [17]. The images used were the color image and 800 × 600 pixels size.

In order to know the proposed method performance, the measurement of success rate in detecting and localizing the iris was performed. Measurement using the accuracy-rate method. This measurement method has been used by [9], [19] using Eq. (4).

$$Acc = \frac{q}{Q} \times 100\% \qquad (4)$$

Where q is the number of detected and localized iris correctly, and Q is the total number of images.

Table 1. Accuracy-rate results

Sesion	Data Number	Localized Number	Accuracy-rate (%)
1	1,214	1,181	97.28
2	663	608	91.70
Total	1,877	1,789	95.31

The measurement result using the accuracy-rate to the proposed method is presented in Table 1. Based on Table 1, the accuracy rate of the proposed method for the image on session 1 is 97.28%, on session 2 is 91.70%, and for all data is 95.31%.

CONCLUSION

It has been presented in this paper the method of iris detection and localization using Contrast Shrinking and Stretching of CIELab Color. Generally, to detect of iris performed on grayscale images or color images are converted to grayscale. The proposed method uses L* and b* channels of the CIELab color model. Channel L* was used to iris detect, and channel b* was used to pupil detect. This method is simple because it does not require a training process or complex calculation, but produces a high level of accuracy-rate (95.31%). Our next studies will focus on iris segmentation as well as eyelid and eyelashes removal from localized image.

REFERENCES

[1] Z. He, T. Tan, and Z. Sun, "Iris Localization via Pulling and Pushing," in The 18th International Conference on Pattern Recognition (ICPR'06), 2006.

[2] J. Liu-jimenez, S. Member, and R. Sanchez-reillo, "Iris Biometrics for Embedded Systems," IEEE Trans. VERY LARGE SCALE Integr. Syst., vol. 19, no. 2, pp. 274–282, 2011.

[3] K. W. Bowyer, K. Hollingsworth, and P. J. Flynn, "Image understanding for iris biometrics: A survey," Comput. Vis. Image Underst., vol. 110, no. 2, pp. 281–307, 2008.

[4] S. E. Hussein, O. A. Hassan, and M. H. Granat, "Assessment of the potential iridology for diagnosing kidney disease using wavelet analysis and neural networks," Biomed. Signal Process. Control, vol. 8, no. 6, pp. 534–541, 2013.

[5] J. Daugman, "Statistical richness of visual phase information: Update on recognizing persons by iris patterns," International Journal of Computer Vision. 2001.

[6] R. P. Wildes, "Iris Recognition: An Emerging Biometric Technology," in PROCEEDINGS OF THE IEEE, 1997, pp. 1348–1363.

[7] A. Ferone, M. Frucci, A. Petrosino, G. Sanniti, and D. Baja, "Iris Detection Through Watershed Segmentation," in Biometric Authentication: First International Workshop, BIOMET 2014, 2014, vol. 8897, pp. 57–65.

[8] F. Yan, Y. Tian, H. Wu, Y. Zhou, L. Cao, and C. Zhou, "Iris segmentation using watershed and region merging," in 2014 9th IEEE Conference on Industrial Electronics and Applications, 2014, pp. 835–840.

[9] F. Jan, I. Usman, S. A. Khan, and S. A. Malik, "Iris localization based on the Hough transform, a radial-gradient operator, and the gray-level intensity," Opt. - Int. J. Light Electron Opt., vol. 124, no. 23, pp. 5976–5985, 2013.

[10] H. Proença, "Iris Recognition: On the Segmentation of Degraded Images Acquired in the Visible Wavelength," IEEE Trans. Pattern Anal. Mach. Intell., vol. 32, no. 8, pp. 1502–1516, 2010.

[11] C. C. Liu, P. C. Chung, C. M. Lyu, J. Liu, and S. S. Yu, "A novel iris segmentation scheme," Math. Probl. Eng., vol. 2014, 2014.

[12] G. Sharma, W. Wu, and E. N. Dalal, "The CIEDE2000 color-difference formula: Implementation notes, supplementary test data, and mathematical observations," Color Res. Appl., vol. 30, no. 1, pp. 21–30, Feb. 2005.

[13] A. Kaur and B. . Kranthi, "Comparison between YCbCr Color Space and CIELab Color Space for Skin Color Segmentation," Int. J. Appl. Inf. Syst., vol. 3, no. 4, pp. 30–33, 2012.

[14] G. Hernandez-Gomez, R. E. Sanchez-Yanez, V. Ayala-Ramirez, and F. E. Correa-Tome, "Natural Image Segmentation Using the CIELab Space," in 2009 International Conference on Electrical Communications and Computers, 2009, no. 5, pp. 107–110.

[15] N. Payet and S. Todorovic, "Hough forest random field for object recognition and segmentation.," IEEE Trans. Pattern Anal. Mach. Intell., vol. 35, no. 5, pp. 1066–79, May 2013.

[16] S. T. Rasmana, Y. K. Suprapto, I. K. E. Purnama, K. Uchimura, and G. Koutaki, "Texture Detection for Letter Carving Segmentation of Ancient Copper Inscriptions," Int. J. Pattern Recognit. Artif. Intell., vol. 31, no. 1, p. 1755002, 2016.

[17] H. Proença and L. A. Alexandre, "UBIRIS: A noisy iris image database," in Springer Lecture Notes in Computer Science – ICIAP 2005: 13th International Conference on Image Analysis and Processing, 2005, pp. 970–977.

[18] T. J. Atherton and D. J. Kerbyson, "Size invariant circle detection," Image Vis. Comput., vol. 17, no. 11, pp. 795–803, 1999.

[19] S. Dey and D. Samanta, "A Novel Approach to Iris Localization for Iris Biometric Processing," Int. J. Biomed. Biol. Eng., vol. 1, no. 5, pp. 293–304, 2007.

[20] Z. He, S. Member, and T. Tan, "Toward Accurate and Fast Iris Segmentation for Iris Biometrics," IEEE Trans. Pattern Anal. Mach. Intell., vol. 31, no. 9, pp. 1670–1684, 2009.